AJNR

Complications of Citrobacter neonatal meningitis: assessment by real-time cranial sonography correlated with CT.

R S Levine, H K Rosenberg, R A Zimmerman and A N Stanford

This information is current as of April 17, 2024.

Complications of *Citrobacter* Neonatal Meningitis: Assessment by Real-Time Cranial Sonography Correlated with CT

Richard S. Levine,[1] Henrietta Kotlus Rosenberg,[2] Robert A. Zimmerman,[1] and Alfred N. Stanford[2]

Real-time cranial sonography via the anterior fontanelle was used serially over a 3- and 6-week period, respectively, to evaluate two infants who developed multicystic encephalomalacia secondary to *Citrobacter* neonatal meningitis. Sonographic findings included heterogeneous parenchymal echogenicity, gyral prominence, periventricular hypoechoic areas from which cystic spaces evolved, and development of hydrocephalus. Serial cranial computed tomography over the same time period confirmed the sonographic observations in each case.

Neonatal bacterial meningitis carries significant morbidity and mortality, despite limited response to early antibiotic therapy. In Gram-negative neonatal bacterial meningitis the mortality is 32%–58% [1–3]. A significant number of surviving infants develop complications that may include severe increased intracranial pressure, ventriculitis with loculation of infection, acute hydrocephalus, abscess, infarction, subdural effusion, multicystic encephalomalacia, and cerebral atrophy. Abnormalities occur in 36%–56% of the surviving children [1–3]. The development of complications is difficult to assess clinically because of the limited neurologic repertoire of the neonate. Computed tomography (CT) was the first noninvasive radiographic method used to document these complications and their evolution [4–7]. Real-time cranial sonography has been useful in both the diagnosis and management of complications of neonatal bacterial meningitis [8–12]. In this report, two infants with *Citrobacter diversus* neonatal meningitis are described. The roles of cranial sonography and CT are compared in identifying and following the development of the white-matter parenchymal necrosis that leads to multicystic encephalomalacia.

Methods

Cranial sonography was performed through the anterior fontanelle on an ATL Mark III real-time sector scanner with a 5 MHz transducer. CT was performed on an EMI 1005 head scanner (60 sec scan time, 8 mm slices, 160 × 160 mm matrix).

Case Reports

Case 1

A male infant, the product of an uncomplicated 35 week pregnancy and delivery, developed a temperature of 38.2°C with an episode of cyanosis and apnea at 9 days of age. Cerebrospinal fluid (CSF) obtained by lumbar puncture revealed turbid yellow fluid containing 14,410 white blood cells/mm³ (100% polys), 20 red blood cells/mm³, glucose 6 mg/dl, and protein 310 mg/dl. Gram stain revealed Gram-negative rods. CSF, urine, and nasopharyngeal cultures grew *Citrobacter diversus*. Cultures of blood grew *E. coli*. At 10 days of age real-time cranial sonography performed via the anterior fontanelle revealed no abnormalities. The next day the patient became less responsive and required intubation. The CSF remained abnormal. Cranial sonography performed on day 12 showed abnormally bright gyri, scattered areas of increased parenchymal echogenicity, and several focal hypoechoic periventricular areas (fig. 1A). By day 18 the patient had become conscious, responsive, and appeared normal on neurologic examination. However, sonography performed on that day showed multiple abnormalities including bilateral hypoechoic areas beneath both lateral ventricles, large hypoechoic areas in both frontal regions, an area of increased echogenicity in the parietal region, and an area of decreased echogenicity in the occipital region. The patient's clinical condition deteriorated on day 20 in association with seizure activity. Sonography performed on day 24 demonstrated an enlargement of the areas of involvement in both the frontal and parietal regions, which were now less echogenic than before. There was also some increase in ventricular size (fig. 1B). CT performed on the same day showed that the ventricles were top normal in size but revealed bifrontal and biparietal occipital white-matter encephalomalacia. Cranial sonography on day 30 showed further increase in size of the hypoechoic spaces and enlargement of the lateral ventricles. Head circumference increased over the ensuing 2 weeks. Sonography on day 50 demonstrated a marked interval enlargement of the lateral ventricles and the presence of very large anechoic bifrontal and parietooccipital areas. The left parietooccipital anechoic area communicated with the occipital horn of the left ventricle (fig. 1C). CT 7 days later showed ventriculomegaly and the presence of bilateral secondary porencephalic cavities in the frontal and parietooccipital regions (fig. 1D).

Case 2

A full-term male infant, the product of an uncomplicated pregnancy and delivery, developed omphalitis and a fever of 38.9°C at 3 days of age. Lumbar puncture revealed cloudy CSF containing 394 white blood cells/mm³ (100% polys), glucose 46 mg/dl, and protein 298 mg/dl. Cultures of CSF grew *Citrobacter diversus*. CT

Fig. 1.—Case 1. **A**, Sonogram, left sagittal view, 12 days of age. Bright midline gyral markings. Debris (D) in left lateral ventricle. Scattered areas of increased parenchymal echogenicity with focal periventricular hypoechoic areas. **B**, Sonogram, left sagittal view, 24 days of age. Slight increase in size of lateral ventricle. Enlargement of left frontal and parietooccipital hypoechoic areas (H). **C**, Sonogram, left sagittal view, 50 days of age. Lateral (LV) and third ventricular dilatation. Marked interval increase in frontal and parietooccipital hypoechoic areas, latter (H) communicating with occipital horn (O). **D**, CT scan, 57 days of age. Ventricular dilatation with marked bilateral frontal and parietooccipital porencephaly.
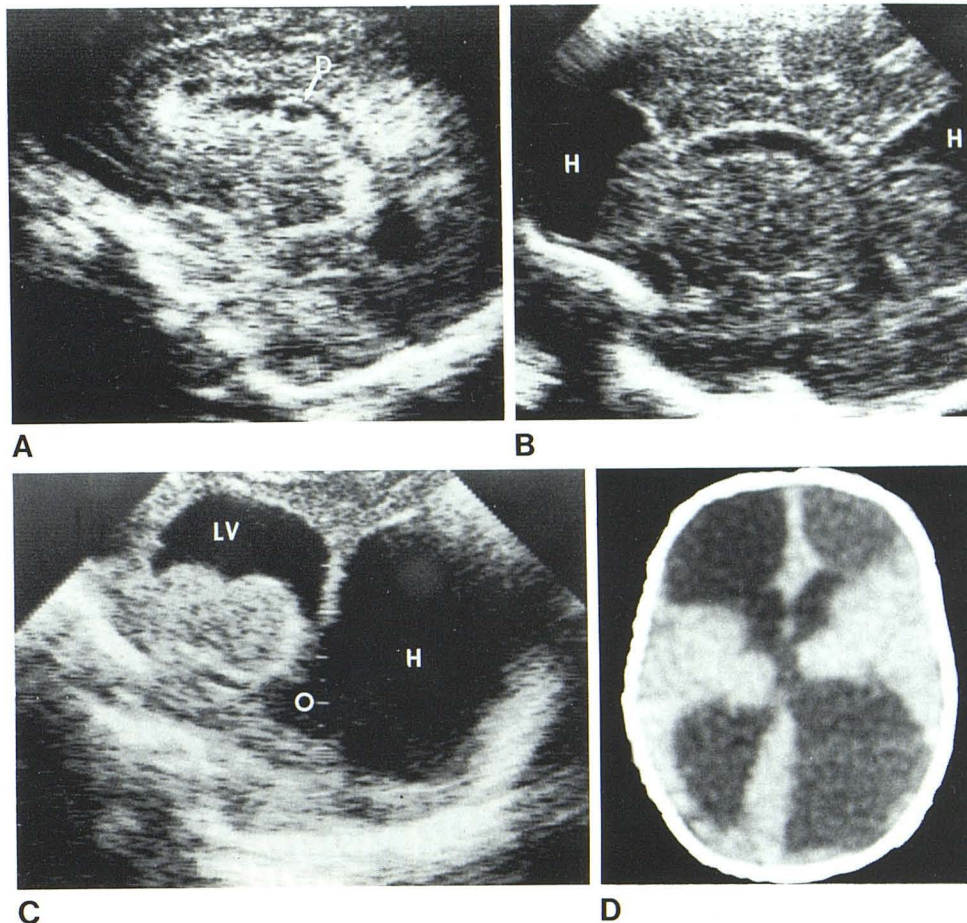
performed on day 6 at the referring hospital appeared normal. Real-time sonography of the brain on day 13 showed slight prominence of the gyri and a diffuse heterogeneous parenchymal pattern. Bilateral focal hypoechoic areas combined with areas of increased and decreased echogenicity were observed above the lateral ventricles. The ventricles were top normal in size (fig. 2A). CT performed on day 14 demonstrated normal-sized ventricles and bifrontal and biparietooccipital encephalomalacia (fig. 2B). Follow-up sonography at 21 days of age showed an enlargement of the ventricles. Further enlargement of frontal and parietal hypoechoic zones was observed on sonography at 29 days of age (fig. 2C). The next day CT demonstrated ventriculomegaly and bilateral frontal and parietooccipital secondary porencephaly (fig. 2D). A subsequent CT examination at 19 weeks of age demonstrated multicystic encephalomalacia.

Discussion

The two most devastating consequences of neonatal bacterial meningitis are parenchymal necrosis and ventricular dilatation of the brain. The necrosis occurs secondary to bacterial vasculitis and resulting infarction. The dilatation results from loss of brain substance after infarction, ventriculitis that leads to scarring of the ventricular outlets (foramen of Monro, cerebral aqueduct, foramina of Luschka and Magendie), and the development of inflammatory septa (obstructive compartmentalized hydrocephalus). Because the clinical neurological evaluation of the neonate is limited in scope, it is essential to use a sensitive diagnostic imaging method that will demonstrate the earliest structural pathology. This may enable the clinician to institute more aggressive therapy in the hope of preventing more damaging sequellae. Previous reports [4, 6, 9] have established the efficacy of both CT and sonography in demonstrating ventricular changes resulting from neonatal bacterial meningitis. Another report [7] has documented the efficacy of CT in demonstrating the evolution of parenchymal encephalomalacia secondary to neonatal bacterial meningitis.

The sonographic studies performed on our two patients have shown that sonography is able to detect mild, diffuse increases in parenchymal echogenicity accompanied by periventricular hypoechoic zones as early as 9–10 days after onset of symptoms, when the ventricles are still normal in size (figs. 1A, 2A). In both patients the periventricular hypoechoic zones became larger and progressively less echogenic during the week after initial detection. These areas correspond to the bilateral parenchymal encephalomalacia demonstrated on CT. As the disease progresses, both sonography and CT demonstrate cavitation of the damaged brain parenchyma with secondary porencephaly (figs. 1C and 2C). Concomitant with the loss of brain substance, ventricular enlargement was obvious on both CT and sonography.

The sonographic observations in these patients included gyral prominence, heterogeneous parenchymal echogenicity, and multi-
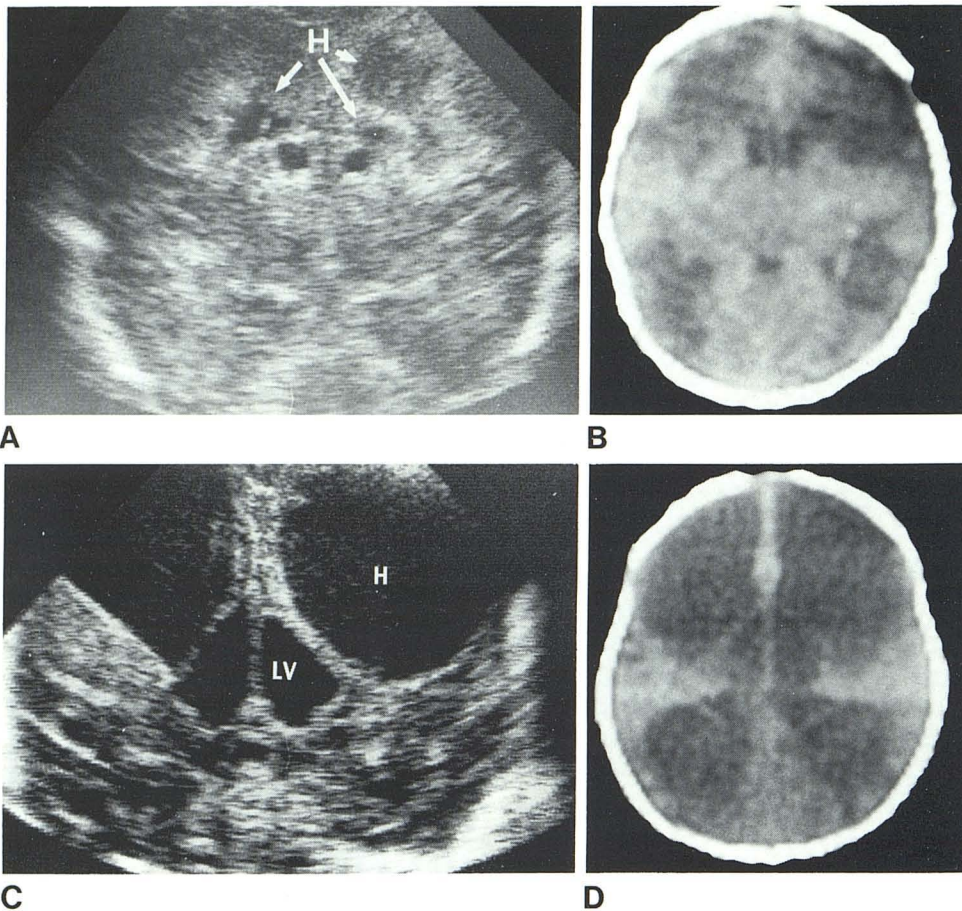
A

B

C

D

Fig. 2.—Case 2. **A**, Sonogram, coronal view, 13 days of age. Slightly prominent midline gyral markings. Parenchyma shows diffuse heterogeneity of echoes with bilateral periventricular hypoechoic areas (H). **B**, CT scan, 14 days of age. Bifrontal and biparietooccipital encephalomalacia with normal ventricles. **C**, Sonogram, coronal view, 29 days of age. Persistent parenchymal heterogenous echogenicity. Marked increase in size of frontal and parietal hypoechoic areas (H) with rim echogenicity and fewer internal echoes. Increase in lateral ventricular (LV) dilatation. **D**, CT scan, 30 days of age. Marked bilateral frontal and parietooccipital secondary porencephaly and ventriculomegaly.

ple areas of decreased echogenicity from which large anechoic spaces evolved. The sulci on the interhemispheric surfaces of the neonatal brain are not visualized sonographically until about 32 weeks of gestational age, becoming more prominent thereafter [13]. While gyral prominence may be normal in full-term infants, excessive brightness may be due to arachnoiditis and subependymal gliosis, noted neuropathologically in the first week of neonatal meningitis [14]. Edwards et al. [12] observed such focal areas of increased cortical echogenicity in six of 20 infants with complicated meningitis.

In the second week after onset of meningitis both infants demonstrated heterogeneous parenchymal echogenicity. This may have resulted from glial reaction subjacent to arachnoiditis, diffuse encephalopathy, or early changes of cerebral infarction, all of which are pathologically observed in the second and third weeks of meningitis [14]. The periventricular hypoechoic areas noted during the second week of meningitis in these patients may represent areas of incipient abscess, infarction, or cerebritis, all of which exhibit an initial low-density appearance on CT [4, 5, 15, 16]. Enzmann et al. [17] observed similar hypoechoic regions in early stages of abscess formation. Unlike the evolution of brain abscess, in which the parenchymal spaces decrease in size, these periventricular areas increased to large anechoic spaces with thin echogenic borders. While *Citrobacter* neonatal meningitis may cause cerebral necrosis with accompanying porencephalic cysts and abscesses [18–20], such parenchymal cysts are not abscesses on postmortem examination [21]. Sonographic differentiation of cysts

and abscesses in infants with complicated meningitis may not be possible on initial evaluation and may require serial studies to assess relative changes in size, central echoes, and borders.

Before the advent of portable high-resolution real-time sonographic equipment, CT was the diagnostic procedure of choice to evaluate patients with complicated neonatal bacterial meningitis. Cranial sonography, performed through an open anterior fontanelle or split sutures, can now provide serial assessment of complications with more rapidity and accessibility and without the expense or ionizing radiation of CT. In our two patients the results of sonography and CT were comparable, with sonography demonstrating parenchymal changes before ventricular dilatation occurred. While long-term outcome of the course of the disease may not be affected by the use of either CT or sonography, correlation of these findings with neuropathologic changes may aid the clinician in prescribing treatment.

REFERENCES

1. Volpe JJ. *Neurology of the newborn.* Philadelphia: Saunders, **1981**:536–571
2. McCracken GH Jr, Mize SG. A controlled study of intrathecal antibiotic therapy in Gram-negative enteric meningitis of infancy. *J Pediatr* **1976**;89:66–72
3. Fitzhardinge PM, Kazemi M, Ramsay M, Stern L. Long-term sequelae of neonatal meningitis. *Dev Med Child Neurol* **1974**;16:3–10

4. Cockrill HH, Dreisbach J, Lowe B, Yamauchi T. Computed tomography in leptomeningeal infections. *AJR* **1978**;130:511–515

5. Bilaniuk LT, Zimmerman RA, Brown L, Yoo HJ, Goldberg HI. Computed tomography in meningitis. *Neuroradiology* **1978**;16:13–14

6. Stovring J, Snyder RD. Computed tomography in childhood bacterial meningitis. *J Pediatr* **1980**;96:820–823

7. Brown LW, Zimmerman RA, Bilaniuk LT. Polycystic brain disease complicating neonatal meningitis: documentation of evolution by computed tomography. *J Pediatr* **1979**;94:757–759

8. Horbar JD, Philip AGS, Lucey JF. Ultrasound scans in neonatal ventriculitis. *Lancet* **1980**;1:976

9. Hill A, Shackelford GD, Volpe JJ. Ventriculitis with neonatal bacterial meningitis: identification by real-time ultrasound. *J Pediatr* **1981**;99:133–136

10. Slovis TL. Real-time ultrasound of the intracranial contents. In: Haller JO, Shkolnik A, eds. *Ultrasound in pediatrics. Clinics in diagnostic ultrasound*, no. 8. New York: Churchill-Livingstone, **1981**:13–27

11. Slovis TL, Kelly JK, Eisenbrey AB, Quiroga A, Greninger N. Detection of extracerebral fluid collections by real-time sector scanning through the anterior fontanelle. *J Ultrasound Med* **1982**;1:41–44

12. Edwards MK, Brown DL, Chua GT. Complicated infantile meningitis: evaluation by real-time sonography. *AJNR* **1982**;3:431–434

13. Rouse GA, Grube GL, Morris RE, Thompson JR, Lu A. Ultrasonography of the developing neonatal brain. Exhibit at the annual meeting of the Radiological Society of North America, Chicago, November **1981**

14. Berman PH, Banker BQ. Neonatal meningitis: a clinical and pathological study of 29 cases. *Pediatrics* **1966**;38:6–24

15. Zimmerman RA, Patel S, Bilaniuk LT. Demonstration of purulent bacterial intracranial infections by computed tomography. *AJR* **1976**;127:155–165

16. Weisberg LA. Cerebral computerized tomography in intracranial inflammatory disorders. *Arch Neurol* **1980**;37:137–142

17. Enzmann DR, Britt RH, Lyons B, Carroll B, Wilson DA, Buxton J. High resolution ultrasound evaluation of experimental brain abscess evolution: comparison with computed tomography and neuropathology. *Radiology* **1982**;142:95–102

18. Gwynn CM, George RH. Neonatal *Citrobacter* meningitis. *Arch Dis Child* **1973**;48:455–458

19. Tamborlane WV Jr, Soto EV. *Citrobacter diversus* meningitis: a case report. *Pediatrics* **1975**;55:739–741

20. Vogel LC, Ferguson L, Gotoff SP. *Citrobacter* infections of the central nervous system in early infancy. *J Pediatr* **1978**;93:86–88

21. Friede RL. Cerebral infarcts complicating neonatal leptomeningitis: acute and residual lesions. *Acta Neuropathol* (Berl) **1973**;23:245–253